Zeitschrift für Kristallographie, Bd. 146, S. 185–203 (1977)

An orthrohombic superstructure of tridymite existing between about 105 and 180°C

By **Kuniaki Kihara**

Department of Earth Sciences, Kanazawa University, Kanazawa 920, Japan

(Received 25 May 1977)

Abstract

A modification of tridymite with an orthorhombic structure exists between monoclinic low tridymite and orthorhombic high tridymite. The three unit-cell edges of this structure are parallel with the corresponding ones of orthorhombic high tridymite but the a translation is three times as long as that of the latter. The crystal structure was determined by the use of x-ray intensities at about 155 °C on a crystal from refractory silica brick. The space group is $P2_12_12_1$ and the unit cell of, dimensions $a = 26.171(3)$, $b = 4.986(4)$ and $c = 8.196(4)$ Å, contains twenty-four formula units. The six-membered rings of the silica tetrahedra are distorted in a way similar to those of monoclinic low tridymite: two thirds have a ditrigonal shape and one third have an oval shape in (001). The same ring types stack on top of one another along the orthorhombic c axis (parallel with the c direction of hexagonal ideal tridymite). This is not the case in monoclinic low tridymite. The mean Si—O distance, uncorrected for thermal motion, is 1.58 Å and the mean values of the Si—O—Si angles are 170.4° for tetrahedra joined nearly parallel to c, and 153.0° for those nearly in (001).

Introduction

Since the x-ray study of single crystals of tridymite at both room temperature and elevated temperatures were made by Buerger and Lukesh (1942), many modifications of tridymite have been suggested. Among such modifications, the crystal structures of monoclinic low tridymite (Dollase and Baur, 1976; Kato and Nukui, 1976) and orthorhombic high tridymite (Dollase, 1967) have been well established to date by x-ray diffraction methods.

Monoclinic low tridymite is known to occur in meteorites (Dollase and Buerger, 1966), in lunar basalts (Dollase *et al.*, 1971; Appelman *et al.*, 1971), in terrestrial dacite (Kawai *et al.*, 1975), in fired silica brick (DOLLASE and BUERGER, 1966), from quartz in sodium tungstate melts (HOFFMANN, 1966) and from silica glass under hydrothermal conditions (KATO and NUKUI, 1976). In this monoclinic structure, the six-membered rings are distorted into two different configurations: two thirds have a ditrigonal shape and one third have an oval shape (DOLLASE and BAUR, 1976).

According to DOLLASE (1967), above about 107 °C low tridymite from the Steinbach meteorite transforms reversibly to a phase which shows a diffraction pattern similar to that of hexagonal high tridymite, but the diffraction maxima are accompanied by satellites in the pseudohexagonal a^* direction, the spacing of which indicates a periodicity that apparently varies continuously from about 105 Å at 107 °C to about 65 Å at 180 °C. Above that temperature, this phase transforms to orthorhombic high tridymite. Satellite reflections along the same direction, with marked diffuse streaks along the pseudohexagonal c^*, were also observed between 120 ° and 180 °C by SATO *et al.* (1977) from synthetic monoclinic low tridymite.

Orthorhombic high tridymite exists above about 180°C and has a small cell dimensionally similar to that of hexagonal high tridymite. In this structure, the framework of silica tetrahedra is slightly distorted from the ideal hexagonal tridymite, while the six-membered rings have hexagonal shape in the (001) projection.

In this study of tridymite from fired silica brick, an orthorhombic superstructure with a $3 \times 1 \times 1$ cell, compared to that of orthorhombic high tridymite, was found in the temperature range about 105 to 180° C; that is, the structural behaviour of the present tridymite as a function of temperature is different from that of meteoritic tridymite. The crystal structure will be discussed and compared with those of monoclinic low tridymite and orthorhombic high tridymite.

Experimental

In scanning electron-microscopic analysis employing an energy-dispersion x-ray detector, there is no indication of any impurity in specimens of tridymite from refractory silica brick. The specimens were monoclinic, space group Aa*, with $a = 25.86(1)$, $b = 4.99(2)$, $c = 18.504(4)$ Å and $\beta = 117.66(1)°$ at room temperature; these

---

* According to DOLLASE and BAUR (1976) and KATO and NUKUI (1976), the space group of monoclinic low tridymite is noncentrosymmetric Cc. In this study, however, Aa is used. This is an equivalent of Cc, but is more convenient in relation to the axial setting of orthorhombic high tridymite.

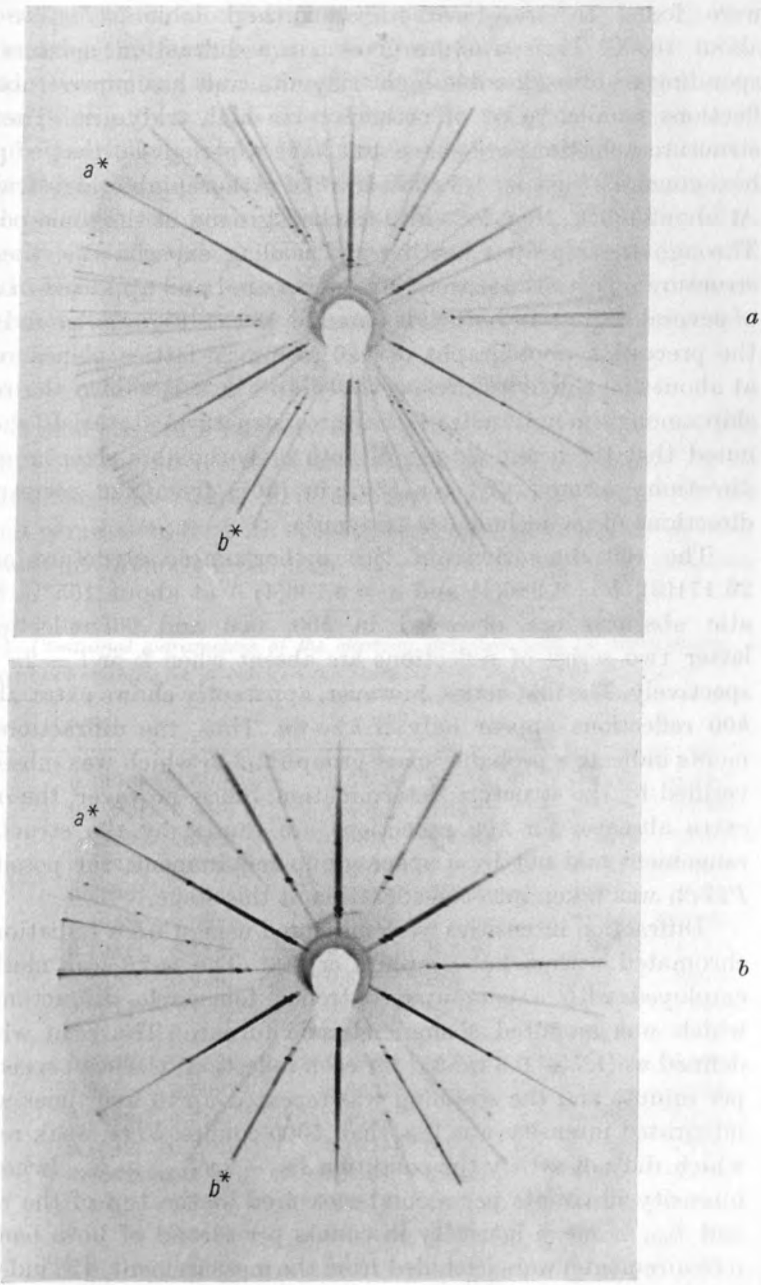

Fig. 1. Precission photographs taken with Mo radiation. *a:* Taken at 150 °C, *b:* Taken at 200 °C. The direction of c^* is perpendicular to the photographs

were found to transform to an orthorhombic structure above about 105 °C. This structure gives x-ray diffraction maxima corresponding to orthorhombic high tridymite and has superstructure reflections parallel to a^* of orthorhombic high tridymite. The superstructure reflections are sharp and have a period 1/6 that of pseudo-hexagonal a^*, that is, 1/3 that of a^* of orthorhombic high tridymite. At about 180 °C, they fade into the background in the same positions. Through the repeated heating and cooling experiments, the superstructure reflections respectively disappeared and appeared in a range of several degrees in both sides around 180 °C. Figures 1*a* and *b* show the precession photographs of $hk0$ reciprocal-lattice planes recorded at about 150 and 200 °C, respectively. In Fig. 2 is shown the relationship among the unit cells of the three structural states. It should be noted that the *a* and *b* axes of both orthorhombic structures are in directions rotated 60° (or 120°) in (001) from the corresponding directions of monoclinic low tridymite.

The cell dimensions of this orthorhombic structure are $a = 26.171(3)$, $b = 4.986(4)$ and $c = 8.196(4)$ Å at about 155 °C. Systematic absences are observed in $h00$, $0k0$ and $00l$ reflections; the latter two series of reflections are absent when k or $l = 2n + 1$ respectively. The first series, however, apparently shows extra absences; $h00$ reflections appear only if $h = 6n$. Thus, the diffraction experiments indicate a probable space group $P2_12_12_1$ which was subsequently verified by the structure determination. Since, however, the observed extra absences for $h00$ reflections are caused by the structural arrangement and not by a space group requirement, the possibility of $P22_12_1$ was taken into consideration at this stage.

Diffraction intensities were measured using Cu$K\alpha$ radiation monochromated with a flat graphite crystal. The ω-2θ scan method was employed with a computer-controlled four-circle diffractometer on which was mounted a small electric furnace. The scan width was defined as $(1.7 + 0.3 \tan\theta)^\circ$ for each reflection; the scan speed was 4° per minute and the scanning was repeated up to five times when the integrated intensity was less than 5000 counts. Very weak reflections which did not satisfy the condition $I_{\text{top}} - 2\sqrt{I_{\text{top}}} \geqslant I_{\text{bck}}$ (where I_{top} is intensity in counts per second measured at the top of the reflection and I_{bck} is mean intensity in counts per second of both background measurements) were excluded from the measurement. 428 independent reflections were measured and 127 were excluded in the region below $\sin\theta/\lambda = 0.46$ Å^{-1}.

The upper limit of the region measured, namely $\theta = 45°$, was determined by the furnace aperture. The crystal was assumed to be spherical in correcting the intensities for Lorentz, polarization factors and absorption effects. The crystal used for intensity measurement had a subequant shape about 0.17 mm in diameter, not platy (smaller or platy fragments apparently showed different and more complicated thermal behaviour in their differential thermal analyses and preliminary x-ray investigations). This crystal had small amounts of other twin individuals up to a maximum of 2% in volume, but this minor imperfection was considered to give a negligible effect on the intensities.

Structure determination and refinement

The crystal structure was solved by applying the key-shift method (Ito, 1973) to the structure of orthorhombic high tridymite. Space groups $P2_12_12_1$ and $P22_12_1$ were assumed; the initial values of the positional parameters for both space groups were transformed directly from those of orthorhombic high tridymite. A key-shift program

Table 1. *Positional parameters of the starting structure and, in parentheses, positional changes in Å between the starting and the refined structures*

Atom	x	y	z
Si(1)	0.1395(0.005)	0.5359(0.370)	0.4386(0.090)
Si(2)	0.1395(−0.050)	0.4641(0.178)	0.0614(0.095)
Si(3)	0.0272(0.020)	0.5359(0.418)	0.5614(0.014)
Si(4)	0.0272(0.029)	0.4641(0.183)	−0.0614(−0.010)
Si(5)	0.1939(0.034)	0.0359(0.393)	0.5614(0.083)
Si(6)	0.1939(−0.002)	−0.0359(0.158)	−0.0614(0.069)
O(1)	0.1945(0.116)	0.0 (0.279)	0.75 (0.112)
O(2)	0.1388(−0.096)	0.5 (0.345)	0.25 (0.090)
O(3)	0.0273(−0.120)	0.5 (0.382)	0.75 (−0.004)
O(4)	0.0833(0.107)	0.5597(0.034)	0.5 (0.162)
O(5)	0.0833(0.052)	0.4403(−0.074)	0.0 (−0.187)
O(6)	0.25 (−0.008)	−0.0597(−0.011)	0.0 (−0.094)
O(7)	0.1682(0.218)	0.3029(0.521)	0.5213(0.201)
O(8)	0.1682(0.248)	0.1971(0.278)	0.0213(0.135)
O(9)	0.1682(−0.314)	0.8029(0.585)	0.4787(0.138)
O(10)	0.1682(−0.260)	0.6971(0.274)	−0.0213(−0.081)
O(11)	0.0 (−0.245)	0.3029(0.572)	0.4787(−0.106)
O(12)	0.0 (−0.245)	0.1971(0.339)	−0.0213(−0.088)

Calculations of positional changes were based on the cell dimensions $a = 26.171$, $b = 4.986$ and $c = 8.196$ Å.

KEY (ITO, 1973) was used. Several iterations based on the $P2_12_12_1$ structure rapidly improved the agreement between observed and calculated structure factors, while the $P22_12_1$ structure was hardly improved. Table 1 lists the initial positional parameters of the structure of $P2_12_12_1$; the positional changes in Å of the structure were determined by least-squares refinement from this starting structure. In this space group there is only one set of equivalent positions; this has 4-fold multiplicity. Accordingly the twenty-four Si atoms were assigned to six independent positions and the forty-eight O atoms were assigned to twelve independent positions.

Least-squares refinement was initiated at the stage of $R = 30\%$, using a local version of the block-diagonal least-squares program HBLS (ASHIDA, 1967). The weighting scheme was defined as $w = 1$ when $|F_o| \leq F_{\max}$ and $w = F_{\max}/|F_o|$ when $|F_o| > F_{\max}$, where $|F_o|$ is an unscaled observed structure factor and $F_{\max}$ is 70 (about

Table 2. *Refined positional and anisotropic temperature parameters* (e.s.d.'s are given in parentheses)

(*a*) Positional parameters

Atom	x	y	z
Si(1)	0.1397(3)	0.6100(13)	0.4496(9)
Si(2)	1376(3)	4998(13)	729(9)
Si(3)	280(3)	6198(13)	5631(9)
Si(4)	283(3)	5008(13)	− 627(9)
Si(5)	1952(3)	1148(13)	5715(9)
Si(6)	1938(3)	− 42(13)	− 530(9)
O(1)	1989(12)	56(4)	764(2)
O(2)	1351(12)	569(5)	261(2)
O(3)	227(10)	577(4)	750(2)
O(4)	0.0874(8)	0.567(4)	0.520(3)
O(5)	853(7)	426(3)	− 23(4)
O(6)	2497(7)	− 62(4)	− 11(3)
O(7)	1765(6)	407(3)	546(2)
O(8)	1777(6)	253(2)	38(3)
O(9)	1562(7)	920(4)	496(3)
O(10)	1583(8)	752(4)	− 31(3)
O(11)	− 94(6)	418(3)	466(3)
O(12)	− 94(7)	265(3)	− 32(2)

Table 2. *(Continued)*

(*b*) Temperature parameters (× 10) of the form

$\exp -(\beta_{11}h^2 + \beta_{22}\,k^2 + \beta_{33}\,l^2 + 2\,\beta_{12}\,hk + 2\,\beta_{13}\,hl + 2\,\beta_{23}\,kl)$.

Atom	β_{11}	β_{22}	β_{33}
Si(1)	0.009(2)	0.12(3)	0.14(2)
Si(2)	008(2)	16(4)	13(2)
Si(3)	011(2)	12(3)	10(2)
Si(4)	009(2)	14(4)	14(2)
Si(5)	009(2)	18(4)	09(2)
Si(6)	010(2)	14(4)	12(2)
O(1)	044(8)	32(13)	12(4)
O(2)	057(10)	70(16)	05(4)
O(3)	048(9)	42(12)	11(5)
O(4)	014(5)	57(13)	40(8)
O(5)	009(4)	16(9)	48(8)
O(6)	004(4)	66(15)	20(5)
O(7)	009(4)	34(10)	15(4)
O(8)	005(4)	31(10)	30(5)
O(9)	016(5)	29(10)	36(7)
O(10)	017(5)	47(12)	24(5)
O(11)	007(4)	29(10)	25(5)
O(12)	012(4)	28(10)	22(5)

Atom	β_{12}	β_{23}	β_{13}
Si(1)	0.002(6)	−0.04(2)	−0.003(5)
Si(2)	− 010(6)	− 00(2)	− 002(4)
Si(3)	002(6)	02(2)	− 003(4)
Si(4)	− 005(6)	04(2)	− 006(5)
Si(5)	008(6)	01(2)	000(4)
Si(6)	− 015(6)	04(2)	002(5)
O(1)	− 05(3)	05(6)	01(2)
O(2)	03(3)	− 10(7)	02(1)
O(3)	02(3)	08(6)	− 01(2)
O(4)	02(2)	− 14(9)	05(2)
O(5)	− 01(2)	− 08(8)	04(2)
O(6)	04(2)	− 01(6)	− 01(1)
O(7)	03(1)	− 07(6)	− 02(1)
O(8)	01(1)	− 12(7)	− 04(1)
O(9)	01(2)	− 19(7)	− 04(2)
O(10)	− 02(2)	− 09(7)	05(1)
O(11)	00(1)	− 04(7)	− 01(1)
O(12)	− 01(2)	05(6)	− 02(1)

Table 3. *Observed and calculated structure factors*

h k l	F_o	F_c	h k l	F_o	F_c	h k l	F_o	F_c	h k l	F_o	F_c	h k l	F_o	F_c	h k l	F_o	F_c
6 0 0	197	225	0 1 1	16	12	10 0 2	4	2	18 0 3	9	9	11 0 4	23	24	10 1 5	18	16
12	20	19	1	3	4	11	20	21	15	3	5	12	38	36	11	6	10
18	154	160	2	35	34	12	54	52	13	16	14	13	10	15	12	7	8
21 1 0	92	99	3	136	129	13	9	14	12	108	110	15	5	6	13	8	12
20	7	12	4	32	35	15	4	7	11	15	19	17	6	9	14	32	32
18	9	11	5	4	1	18	99	96	7	12	13	18	12	15	15	86	90
16	40	39	6	13	14	19	19	10	6	110	105	19	14	16	16	35	31
15	85	82	7	4	2	21	4	5	5	18	14	17 1 4	2	3	13 2 5	29	26
14	58	59	8	33	29	21 1 2	72	70	1	5	5	16	10	16	12	67	70
13	6	4	9	32	28	20	16	11	0 1 3	5	3	15	27	24	11	44	46
12	35	35	10	36	35	18	9	10	2	18	13	14	18	20	10	15	15
11	8	7	12	15	16	16	27	29	3	83	77	13	5	4	9	17	19
10	91	93	13	6	6	15	51	51	4	10	13	12	8	8	8	15	15
9	138	134	14	30	27	14	37	39	5	2	10	11	6	7	7	48	46
8	93	89	15	74	71	13	8	6	6	5	6	10	25	18	6	80	81
7	11	9	18	8	7	12	20	23	8	15	16	9	31	29	5	47	46
6	40	39	20	11	13	11	9	6	9	16	15	8	15	24	4	13	12
5	9	8	21	53	53	10	49	46	10	24	23	7	5	7	3	15	15
4	66	65	22	12	7	9	35	36	11	5	8	6	10	8	2	11	8
3	194	205	19 2 1	36	39	8	39	44	12	11	8	5	7	8	1	31	33
2	38	35	18	91	86	7	6	3	13	6	6	4	32	27	0	29	28
0 2 0	165	168	17	53	51	6	18	16	14	29	32	3	101	97	0 3 5	23	22
1	58	55	16	8	9	5	6	6	15	103	104	2	37	36	1	18	18
2	5	4	15	24	23	4	35	32	16	36	29	1	10	11	2 3 5	52	56
3	20	21	14	7	6	3	122	115	17	5	4	0	13	14	3	22	20
4	4	2	13	54	56	2	35	35	18	12	11	0 2 4	29	29	4	50	51
5	27	26	12	62	60	1	6	6	19	5	9	1	15	10	5	15	17
6	13	10	11	58	58	0	14	14	20	20	24	2	7	8	6	16	15
7	6	7	10	7	7	0 2 2	53	54	18 2 3	45	39	3	11	13	7	11	9
8	3	9	9	24	22	1	15	12	17	23	20	4	10	8	0 0 6	95	95
9	12	11	8	7	6	2	3	2	15	10	12	5	42	42	1	28	19
10	5	6	7	47	46	3	11	12	14	5	8	6	65	65	2	6	6
11	43	44	6	81	74	4	5	9	13	27	33	7	44	47	4	3	2
12	50	49	5	40	40	5	35	37	12	74	74	8	13	12	5	13	15
13	55	59	4	3	3	6	56	55	11	45	46	9	19	19	6	52	52
14	8	3	3	13	14	7	40	42	10	9	14	10	11	9	7	20	7
15	29	27	1	7	6	8	7	11	9	18	19	11	41	35	8	5	2
16	7	5	0	92	93	9	19	19	8	8	9	12	55	52	10	6	7
17	58	57	0 3 1	21	20	10	7	8	7	35	32	13	37	36	11	24	9
18	96	101	1	5	6	11	43	40	6	77	72	14	10	8	12	47	55
19	41	40	2	50	53	12	51	49	5	33	33	15	10	13	13	4	22
20	4	4	3	85	80	13	44	44	4	5	9	16	7	6	12 1 6	3	5
21	13	14	4	63	66	14	9	9	3	11	11	12 3 4	11	13	11	8	4
16 3 0	14	15	5	8	5	15	19	17	2	5	5	11	4	3	10	30	25
15	19	23	6	33	32	16	7	6	1	13	14	10	18	20	9	87	90
14	29	26	7	9	5	17	37	34	0	34	37	8	20	18	8	31	29
12	22	20	8	81	84	18	65	65	0 3 3	18	18	7	7	7	7	8	4
11	7	6	9	71	68	19	23	24	1	8	7	6	15	15	6	6	9
10	57	61	10	78	77	16 3 2	42	43	2	36	37	5	12	14	5	7	3
9	39	37	11	9	7	15	40	37	3	49	45	4	58	56	4	23	23
8	61	61	12	29	29	14	40	38	4	44	42	3	49	50	3	60	58
7	7	9	13	7	4	13	7	7	5	9	10	2	72	71	2	21	22
6	27	28	14	47	48	12	15	17	6	17	17	1	21	21	1	6	6
4	42	35	15	81	76	10	26	28	7	9	14	0	31	32	0	5	8
3	32	37	16	21	21	9	18	17	8	35	37	13 0 5	23	19	0 2 6	40	49
2	24	24	9 4 1	8	10	8	26	24	9	28	27	12	108	106	1	39	41
0 4 0	8	6	8	6	6	7	4	4	10	32	32	11	31	31	2	15	13
1	3	9	7	50	48	6	15	15	11	6	3	10	4	4	3	12	13
5	7	5	6	29	26	5	6	12	12	11	10	7	28	30	4	12	14
6	10	9	5	73	76	4	49	48	14	23	22	6	135	135	5	29	32
7	12	7	4	10	11	3	45	44	4 4 3	6	12	5	37	33	6	35	39
8	3	2	3	43	45	2	61	61	3	18	18	4	4	3	7	24	22
9	7	7	2	12	9	1	11	8	2	8	11	1	4	7	8	7	9
20 0 1	1	1	1	103	107	0	29	29	1	43	45	0 1 5	12	10	6 0 7	14	13
18	9	6	0	16	15	0 4 2	6	6	0 0 4	146	136	1	9	12	5	8	13
13	9	9	0 0 2	281	298	1	18	16	1	26	22	2	37	38	2 1 7	2	3
12	91	85	1	27	16	3	14	14	5	16	12	3	108	110	3	12	13
11	2	7	5	16	14	4	6	8	6	38	34	4	32	27	4	7	3
10	2	0	6	101	98	5	47	45	7	8	22	5	7	11			
7	8	10	7	3	19	6	16	15	8	5	11	6	5	4			
6	137	134	9	6	5	7	55	57	9	7	9	8	5	4			
5	6	6	16 1 1	27	27	8	8	10	10	6	5	9	28	31			

50 on an absolute scale): this value seemed to give a reasonable weighting scheme. The atomic scattering factors were taken from International Tables for X-ray Crystallography (1974). In the initial stage of refinement a scale factor, all 54 positional, and 18 isotropic temperature parameters were refined; in the next stage the scale factor and 108 anisotropic temperature factors for all atoms were refined. The final R value was 8.2%.

Difference Fourier maps were computed, based on the parameters obtained at the stage of the refinement for the isotropic temperature factors and the final parameters with anisotropic temperature factors. In the first map small peaks are located near the atomic centers. The vectors from the atoms to their neighbouring peaks approximately corresponded to the root mean-square amplitudes along the longest principal axes of the corresponding thermal ellipsoids described in the next section. Accordingly it was reasonably concluded that the residual peaks could be attributed to anisotropic thermal motion. They disappeared in the map computed using the final parameters with the anisotropic temperature factors. The successful structure determination and the difference maps give strong supports to the choice of the space group $P2_12_12_1$. The atomic coordinates and the temperature coefficients are listed in Table 2. In Table 3 are listed observed and calculated structure factors.

Discussion of the structure

As shown above, the present structure is derived by displaying the atoms in orthorhombic high tridymite. It is apparent from Table 1 that positional changes along b (mean 0.300 Å) are, in general, larger than those along a or c (mean 0.121 or 0.098 Å respectively). For Si atoms, especially, positional changes along b (mean 0.283 Å) are quite large compared with those along a and c (mean 0.023 and 0.060 Å). The positional changes of O atoms, on the other hand, are generally large along b and a and small along c. Such displacements of the O atoms are more effectively illustrated in Fig. 3 where the framework of the silica tetrahedra is projected along c. The six-membered rings of the silica tetrahedra form two different shapes, i.e., for a tridymite layer, two of the six rings in the unit cell have oval shapes and four have ditrigonal shapes. Thus, the configuration of the six-membered rings in each tridymite layer is similar to that in monoclinic low tridymite. Dollase and Baur (1976) indicate these distorted six-membered rings by employing the letters D for ditrigonal, O for oval,

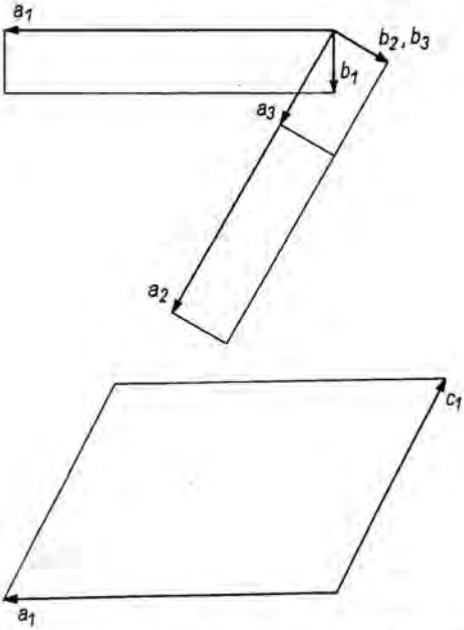

Fig. 2. The relationship among the unit cells of monoclinic low tridymite (1), the present structure (2), and orthorhombic high tridymite (3)

with primes indicating the second of the two possible orientations of each of these ring types. Using these letters, the sequence of the oval and ditrigonal rings in each tridymite layer is expressed as $\cdots DDOD' D'O' \cdots$ along *a* for both structures. In the present structure, the same type rings repeat along *c*, forming ditrigonal and oval channels along *c*, while in monoclinic low tridymite, different type rings stack on preceding ones.

Interatomic distances and angles calculated using a program RSDA4 (SAKURAI, 1967) are listed in Table 4. Individual Si–O distances are within the range 1.50 Å to 1.65 Å, and six independent silica tetrahedra have mean Si–O bond lengths ranging from 1.54 Å to 1.61 Å. Deviations of Si–O distances from the mean values of the individual tetrahedra are up to 4 e.s.d.'s for the Si(l) tetrahedron and 2 e.s.d.'s for the Si(3) and Si(5) tetrahedra. The values of O–Si–O bond angles range from 99.9° to 119.2° (mean 109.4°). This suggest that some tetrahedra deviate from a regular tetrahedron: the maximum deviation is larger for the present structure than that of orthorhombic high tridymite. The mean distance for all twenty-four Si–O distances

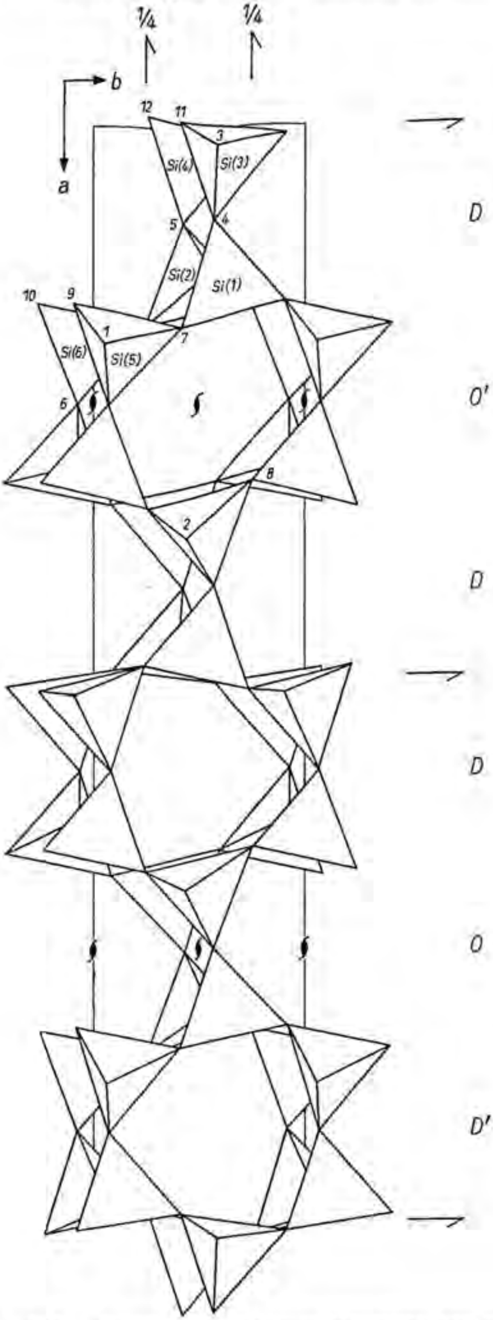

Fig. 3. The framework of silica tetrahedra in the new structure, projected along c. Numbers identify the oxygen atoms

is 1.58 Å which lies between 1.56 Å for orthorhombic high tridymite (DOLLASE, 1967) and 1.60 Å for monoclinic low tridymite (DOLLASE and BAUR, 1976 and KATO and NUKUI, 1976). Si–O–Si bonds may be divided into two groups: one nearly in (001), forming the tridymite layer, and the other nearly in the *c* direction, connecting each tridymite layer. The angles fall in the ranges 147.9° to 159.7° except for Si(5)—O(6)—Si(6) (168.0°) for the former and 168.1° to 171.5° for the latter. The Si(5)—O(6) and Si(6)—O(6) bonds constitute a part of the six-membered rings with oval shape, and the angle 168.0° approximates to the corresponding angles in orthorhombic high tridymite (171.2°). It is then suggested that the tetrahedra of Si(5) and Si(6) are rotated approximately in (001) as a unit around O(6) atoms therby distorting the six-membered rings to oval shape, but keeping the Si—O—Si angle unaltered through the transition. The mean values for the Si—O—Si(⊥) and Si-O-Si(⊥) bond angles are compared with the corresponding ones calculated from the structural data for monoclinic low tridymite (DOLLASE and BAUR, 1976), orthorhombic high tridymite (DOLLASE, 1967) and hexagonal ideal tridymite as follows:

	Monoclinic low tridymite	Present structure	Orthorhombic high tridymite	Hexagonal ideal tridymite
Si—O—Si(∥)	148.0°	153.0°	168.2°	180°
Si—O—Si(⊥)	155.0°	170.4°	178.7°	180°

Table 4. *Interatomic distances and angles*
(e.s.d.'s are given in parentheses)

Si—O distances

Si(1)		Si(2)		Si(3)	
O(2)	1.56(2) Å	O(2)	1.58(2) Å	O(3)	1.55(2) Å
O(4)	1.50(2)	O(5)	1.62(3)	O(4)	1.62(3)
O(7)	1.60(2)	O(8)	1.64(2)	O(11)	1.61(2)
O(9)	1.65(2)	O(10)	1.61(3)	O(11)iii	1.58(2)
mean	1.580	mean	1.614	mean	1.590
Si(4)		**Si(5)**		**Si(6)**	
O(3)	1.59(2) Å	O(1)	1.60(2) Å	O(1)	1.54(2) Å
O(5)	1.57(2)	O(7)	1.55(2)	O(6)	1.53(2)
O(12)	1.55(2)	O(9)	1.54(2)	O(8)	1.54(2)
O(12)iii	1.61(2)	O(6)	1.62(2)	O(10)	1.54(3)
mean	1.581	mean	1.578	mean	1.537

Table 4. *(Continued)*

O–O distances and O–Si–O angles

			Distances	O–Si–O angles
Si(1)	O(2)	O(4)	2.46(4) Å	106.8(1.5)°
	O(2)	O(9)	2.66(3)	111.6(1.3)
	O(2)	O(7)	2.70(3)	116.8(1.2)
	O(4)	O(7)	2.47(3)	105.6(1.2)
	O(4)	O(9)	2.53(3)	106.6(1.2)
	O(7)	O(9)	2.64(3)	108.7(1.0)
Si(2)	O(2)	O(5)	2.76(4)	119.2(1.5)
	O(2)	O(8)	2.66(3)	111.1(1.3)
	O(2)	O(10)	2.63(3)	111.1(1.3)
	O(5)	O(8)	2.62(3)	106.4(1.0)
	O(5)	O(10)	2.51(3)	101.8(1.2)
	O(8)	O(10)	2.60(3)	106.1(1.1)
Si(3)	O(3)	O(11)	2.60(3)	110.3(1.2)
	O(3)	O(11)iii	2.48(3)	104.5(1.2)
	O(3)	O(4)	2.53(3)	106.2(1.4)
	O(4)	O(11)	2.68(3)	111.8(1.1)
	O(4)	O(11)iii	2.69(3)	114.7(1.1)
	O(11)	O(11)iii	2.60(3)	109.0(1.0)
Si(4)	O(3)	O(5)	2.60(4)	110.2(1.5)
	O(3)	O(12)	2.52(3)	106.1(1.2)
	O(3)	O(12)iii	2.52(3)	104.1(1.1)
	O(5)	O(12)	2.60(3)	112.8(1.1)
	O(5)	O(12)iii	2.65(3)	112.8(1.1)
	O(12)	O(12)iii	2.60(3)	110.3(1.1)
Si(5)	O(1)	O(7)	2.57(3)	108.9(1.1)
	O(1)	O(9)	2.56(3)	108.8(1.4)
	O(1)	O(6)iv	2.63(3)	109.2(1.4)
	O(6)iv	O(7)	2.63(3)	112.1(1.0)
	O(6)iv	O(9)	2.56(3)	108.6(1.2)
	O(7)	O(9)	2.52(3)	109.2(1.0)
Si(6)	O(1)	O(6)	2.35(3)	99.9(1.5)
	O(1)	O(8)	2.52(3)	109.5(1.2)
	O(1)	O(10)	2.50(3)	108.6(1.3)
	O(6)	O(8)	2.49(3)	108.2(1.1)
	O(6)	O(10)	2.57(3)	113.8(1.2)
	O(8)	O(10)	2.61(3)	115.7(1.1)

Table 4. (*Continued*)

Si—O—Si angles

Si(1)	O(4)	Si(3)	159.7(1.7)°
	O(9)	Si(5)	148.9(1.4)
	O(7)	Si(5)	147.9(1.2)
	O(2)	Si(2)	171.5(2.0)
Si(2)	O(5)	Si(4)	147.9(1.4)
	O(8)	Si(6)	152.0(1.3)
	O(10)	Si(6)	151.4(1.5)
Si(3)	O(3)	Si(4)	168.1(1.9)
	O(11)	Si(3)iii	147.9(1.3)
Si(4)	O(12)	Si(4)iii	153.3(1.4)
Si(5)	O(1)	Si(6)	171.5(2.3)
	O(6)	Si(6)	168.0(1.7)

Here, ($\|$) and ($\perp$) refer to the Si—O bonds approximately parallel to the layers and nearly perpendicular to the layers respectively, and each value is averaged. It can be seen that flexures of Si—O—Si($\|$) angles are always larger than those of Si—O—Si($\perp$), except for a case of hexagonal ideal tridymite. In orthorhombic high tridymite the tetrahedra joined along *c* are tilted (without largely changing the Si—O—Si angles from 180°) around two-fold rotation axes along *a* and passing through the O atoms bridging two tetrahedra. In other words, the tilting occurs in (100), and the sense of the tilt alternates along *c*. Such tilting results a slight flexure of these Si—O—Si($\|$) bonds, while the Si—O—Si($\perp$) bonds are unaltered. The alternate tilting of tetrahedra is also seen in the present structure and in addition to that, flexures of some pairs of tetrahedra joined nearly in (010), e.g., those joined by O(4), O(5), O(7), O(8), O(9) and O(10), predominate in (001), resulting in oval and ditrigonal distortions. This kind of distortion may be a predominant origin for contraction of the cell-edge lengths, particularly in the *b* and *a* directions.

The cell dimensions measured using a single-crystal diffractometer are

$\mathrm{a} = 26.171(3)$, $b = 4.986(4)$ and $c = 8.196(4)$ Å at about 155 °C,
$a = 26.186(2)$, $b = 4.985(4)$ and $c = 8.204(4)$ Å at about 183 °C,
$a = 8.75\ (1)$, $b = 5.03\ (1)$ and $c = 8.211(5)$ Å at about 220 °C,

where the first two measurements are for the present structure and the last for orthorhombic high tridymite. The *b*-edge lengths are equal within 1 e.s.d. for these temperatures in the region of the present structural state, but they are obviously shorter than that at about 220 °C. This suggests that the cell-edge length varies rapidly in a narrow temperature range around the transition. Such a rapid change is also suggested for the *a* edge length. The temperature dependence of the cell dimensions for the tridymite structure may be interpreted mainly in terms of the angular distortion of the Si—O—Si bonds. If the mean atomic positions approach continuously those of orthorhombic high tridymite with increasing temperature, the cell dimensions also may be continuously lengthened. The behaviour of the cell dimensions observed in the region of the present structural state seems to support an assumption that the mean atomic positions vary little over the great part of the region of this structural state and rapidly approach those of orthorhombic high tridymite at a temperature directly below the transition.

Table 5 gives the mean-square displacements of thermal motions and the relation of the principal axes of the thermal ellipsoids to the crystallographic axes. Thermal motions are apparently large and anisotropic, particularly for the O atoms. The ellipsoids of thermal vibration for the O atoms are nearly oblate or prolate spheroides, the longest axes of which are approximately perpendicular to the Si—O bonds and the shortest axes are nearly parallel to the bonds. The mean-square displacements of the Si and O atoms averaged for three directions, $\langle u^2 \rangle = 1/3(\langle u_{11} \rangle^2 + \langle u_{22} \rangle^2 + \langle u_{33} \rangle^2)$, are compared with those in other tridymite as follows: 0.010 and 0.025 Å^2 for monoclinic low tridymite (KATO and NUKUI, 1976), 0.030 and 0.067 Å^2 for the present structure and 0.040 and 0.106 Å^2 for orthorhombic high tridymite (DOLLASE, 1967), where each value is averaged over all Si and O atoms in each structure. The high anisotropy in O atoms may be caused by static distribution around the mean positions. In comparison with the changes of the mean atomic positions in the present structure from orthorhombic high tridymite, the root mean-square thermal amplitudes of some of the atoms are larger than these displacements.

Because of the large apparent motions described above, it may be expected that averaged instantaneous distances significantly differ from those between the individual averaged positions. Lower and upper limits of the mean separations for the Si—O bonds were estimated,

Table 5. *Mean-square displacements of the atoms along the principal axes;* 1, 2 and 3, of the thermal ellipsoids and the orientations of the principal axes with respect to crystallographic axes; *a*, *b* and *c*

	$\langle u_{ii}^2 \rangle$	*a*	*b*	*c*
Si(1)				
1	0.0311 Å^2	10.6°	91.6°	79.5°
2	0.0129	90.8	13.3	76.8
3	0.0499	100.6	103.2	17.0
Si(2)				
1	0.0317	29.5	118.4	82.7
2	0.0164	61.6	28.4	88.0
3	0.0433	97.4	88.3	7.6
Si(3)				
1	0.0402	33.0	92.8	122.9
2	0.0139	95.5	14.7	103.6
3	0.0331	57.5	75.6	36.3
Si(4)				
1	0.0291	19.5	90.4	70.5
2	0.0152	85.1	13.8	102.9
3	0.0526	108.9	76.2	23.7
Si(5)				
1	0.0343	29.7	64.0	76.8
2	0.0200	113.0	26.9	103.1
3	0.0292	107.7	83.8	18.8
Si(6)				
1	0.0397	22.7	108.7	77.7
2	0.0113	68.4	26.3	104.2
3	0.0446	96.5	72.2	19.0
O(1)				
1	0.1606	14.9	104.7	87.5
2	0.0241	76.5	37.2	123.9
3	0.0502	83.8	56.7	34.0
O(2)				
1	0.2016	10.5	82.0	83.2
2	0.0926	95.7	18.5	107.5
3	0.0070	98.9	73.5	18.9
O(3)				
1	0.1695	8.7	82.8	94.7
2	0.0634	93.2	35.5	54.7
3	0.0246	82.0	124.5	35.7

Table 5. (*Continued*)

	$\langle u_{ii}\rangle^2$	a	b	c
O(4)				
1	0.0116 Å²	36.9°	113.9°	116.4°
2	0.0779	62.6	27.5	88.9
3	0.1674	67.3	102.7	26.4
O(5)				
1	0.0215	35.0	119.7	106.7
2	0.0174	59.5	30.6	92.0
3	0.1767	74.6	96.7	16.9
O(6)				
1	0.0030	19.7	108.6	83.7
2	0.0936	70.5	21.5	98.8
3	0.0684	93.0	79.6	10.8
O(7)				
1	0.0101	33.2	116.5	71.4
2	0.0817	57.6	57.0	130.2
3	0.0329	83.4	44.7	46.0
O(8)				
1	0.0015	22.2	88.9	67.8
2	0.0310	97.1	16.5	75.2
3	0.1275	111.0	106.4	27.1
O(9)				
1	0.0423	39.1	127.5	80.7
2	0.0142	61.4	42.6	61.5
3	0.1563	114.2	107.1	30.3
O(10)				
1	0.0184	38.6	91.8	128.5
2	0.0513	77.6	17.9	77.2
3	0.1291	54.1	107.8	41.4
O(11)				
1	0.0236	8.9	92.3	81.4
2	0.0353	89.0	8.5	81.5
3	0.0886	98.8	98.2	12.1
O(12)				
1	0.0360	54.4	130.7	60.9
2	0.0280	46.5	44.5	82.4
3	0.0888	115.7	75.1	30.3

employing the BUSING and LEVY's method (1964). The corrected bond-length limits averaged for all twenty-four Si—O bonds are 1.59 and 1.71 Å for lower and upper limits respectively. If riding motion is assumed, the mean value is 1.61 Å, which is in better agreement with 1.61 Å (DOLLASE, 1967) or orthorhombic high tridymite and 1.610 Å (KATO and NUKUI, 1976) of monoclinic low tridymite.

Acknowledgement

The author is grateful to Mr. K. SAKAI and Mr. T. ONO, Asahi Glass Research Laboratory, for supplying the tridymite crystals. Thanks are also due to Dr. N. KOHYAMA, National Institute of Industrial Health, Ministry of Labor, for supplying S.E.M. and D.T.A. data for the present tridymite crystals and to Dr. T. MATSUMOTO for reading the manuscript. Dr. T. MATSUMOTO allowed me to use a key shift program KEY introduced to Kanazawa by him. A local version of least-squares program HBLS was kindly supplied by Dr. M. Matsui Kanazawa Medical University. Professor S. SUGIURA encouraged the author throughout this study. The author is indebted to Mr. K. NAKAMURA for taking photographs of the illustrations. The computations were performed at both computer centers of Kanazawa Univ. and Tokyo University.

Note added in proof. A structure of terrestrial triclinic tridymite was reported by KONNERT and APPLEMAN (1978) in the last issue of Acta Crystallogr. (B 34, 391—403).

References

D. APPLEMAN, H. NISSEN, D. STEWART. J. CLARK, E. DOWTY and J. HUEBNER (1971), Studies of lunar plagioclase, tridymite and cristobalite. Proc. 2nd Lunar Sci. Conf. **1**, 117—133.

T. ASHIDA (1967), Universal crystallographic computation program system (UNICS), edited by T. SAKURAI, Cryst. Soc. Japan.

M. J. BUERGER and J. LUKESH (1942), The tridymite problem. Science **95**, 20—21.

W. R. BUSING and H. A. LEVY (1964), The effect of thermal motion on the estimation of bond lengths from diffraction measurements. Acta Crystallogr. **17**, 142—146.

W. A. DOLLASE (1967), The crystal structure at 220°C of orthorhombic high tridymite from the Steinbach meteorite. Acta Crystallogr. **23**, 617—623.

W. A. DOLLASE and M. J. BUERGER (1966), Crystal structure of some meteoritic tridymites. (Abstr.) Geol. Soc. Amer. Prog. 1966, Annu. Meet. 54—55 (not seen but noted by DOLLASE, 1967).

W. A. Dollase, R. A. Cliff and G. W. Wetherill (1971), Note on tridymite in rock 12021. Proc. 2nd Lunar Sci. Conf. **1**, 141–142.

W. A. Dollase and W. H. Baur (1976), The superstructure of meteoritic low tridymite solved by computer simulation. Amer. Mineral. **61**, 971–978.

W. Hoffmann (1967), Gitterkonstanten und Raumgruppe von Tridymit bei 20 °C. Naturwiss. **54**, 114.

J. A. Ibers and W. C. Hamilton (1974), *International tables for x-ray crystallography*, Vol. IV. Kynoch Press, Birmingham.

T. Ito (1973), On the application of a minimum residual method to the structure determination of superstructures. Z. Kristallogr. **137**, 399–411.

K. Kato and A. Nukui (1976), Die Kristallstruktur des monoklinen Tief-Tridymits. Acta Crystallogr. B **32**, 2486–2491.

K. Kawai, T. Matsumoto and K. Kihara (1975), Monoclinic tridymite from Yugawara, Kanagawa Prefecture, Japan. (Abstr.). Mineral. Soc. Japan, Annu. Meet. 45.

T. Sakurai (1967), Universal crystallographic computation program system (UNICS), edited by T. Sakurai, Cryst. Soc. Japan.

M. Sato, J. Löns and W. Hoffmann (1977). (In preparation.)